Field-dependent specific-heat of the pure and diluted 4f electron system Yb4As3

R. Matysiak, G. Kamieniarz, Philipp Gegenwart, H. Aoki, A. Ochiai

Angaben zur Veröffentlichung / Publication details:

Matysiak, R., G. Kamieniarz, Philipp Gegenwart, H. Aoki, and A. Ochiai. 2007. "Field-dependent specific-heat of the pure and diluted 4f electron system Yb4As3." *Inorganica Chimica Acta* 360 (13): 3955–58. https://doi.org/10.1016/j.ica.2007.06.015.

Field-dependent specific-heat of the pure and diluted 4f electron system Yb_4As_3

R. Matysiak [a,*], G. Kamieniarz [b,c], P. Gegenwart [d], H. Aoki [e], A. Ochiai [e]

[a] *Institute of Engineering and Computer Education, University of Zielona Góra, ul. prof. Z. Szafrana 4, 65-516 Zielona Góra, Poland*
[b] *Max Planck Institute for the Physics of Complex Systems, 01187 Dresden, Germany*
[c] *Computational Physics Division, Institute of Physics, A. Mickiewicz University, ul. Umultowska 85, 61-614 Poznań, Poland*
[d] *Max-Planck-Institute for the Chemical Physics of Solids, 01187 Dresden, Germany*
[e] *Center for Low Temperature Science, Tohoku University, Sendai 980-8578, Japan*

Paper presented in the MAGMAMet-ECMM, European Conference on Molecular Magnetism, that took place last October 10–15 in Tomar, Portugal.

1. Introduction

One-dimensional systems have attracted the interest of chemists and physicists for more than three decades. The theory of the ideally uniform $S = 1/2$ antiferromagnetic Heisenberg chain in the magnetic field is well established and usually well describes the properties observed in real systems. The majority of these systems are organic and inorganic compounds with chains of 3d and 4f ions. Recently, a new class of rare-earth pnictide compounds like Yb_4As_3 have become the focus of attention. This compound belongs to a family of R_4X_3 (R = rare-earth, X = As, Bi, P, Sb) compounds of the anti-Th_3P_4 structure [1]. The Yb-ions occupy the phosphorus sites at the three-fold symmetry axes and the As-ions are located at the thorium sites.

At high temperatures (above $T_{CO} \approx 295$ K) Yb_4As_3 has a cubic crystal structure with a lattice constant $a = 8.788$ Å and is a homogeneous intermediate valent (IV) metal with a valence ratio of $Yb^{2+}/Yb^{3+} = 3{:}1$ where the Yb ions reside statistically on four equivalent families of chains along the space diagonals of a cube [2]. At low temperatures, Yb_4As_3 is semimetallic with extremely low carrier concentration of 10^{-3} As-4p holes per a formular unit [3]. The Yb^{3+} ion has one hole in the $4f$ closed shell and forms a one-dimensional spin $S = 1/2$ chain along the $\langle 1\,1\,1\rangle$ direction. The remaining Yb ions take non-magnetic divalent states. The $J = 7/2$ ground multiplet splits into four doublets as a result of the crystal field effect. Thus the low-temperature dynamics is described by an effective $S = 1/2$ spin chain. The neutron scattering experiments on Yb_4As_3 have actually confirmed that the excitation

* Corresponding author.
E-mail address: r.matysiak@eti.uz.zgora.pl (R. Matysiak).

spectrum is well described by the one-dimensional $S = 1/2$ isotropic Heisenberg model [4] in the absence of magnetic field. The interchain interactions are small and ferromagnetic, leading to a low-T spin-glass freezing [5].

Although the system in low-temperatures and in the absence of a magnetic field exhibits a typical heavy-fermion behaviour with linear specific heat coefficient $\gamma \approx 200$ [mJ/(K^2 mol)], finally it has been attributed to 1D spin excitations in the Yb^{3+} chains [5,6]. Moreover, under a magnetic field, the gap in the spin excitation spectrum of Yb_4As_3 opens and obeys the power law $H^{2/3}$ [7], which gives a strong experimental evidence for the existence of a staggered field alternating along the Yb^{3+} chains induced by the Dzyaloshinskii–Moriya interaction as suggested by the sine-Gordon model [8] and observed also in copper benzoate [9] and copper pyrimidine complex [10]. The system seems also interesting as a candidate for the anomalous electron spin resonance behaviour [11,12].

2. The model and simulation technique

Computer modelling of the finite-temperature properties of the Yb_4As_3 is based on the $S = 1/2$ anisotropic Heisenberg model with the antisymmetric Dzyaloshinskii–Moriya interaction [13,14]:

$$\mathcal{H} = -\Bigg\{ J \sum_{i=1}^{N} [\hat{\mathcal{S}}^z_i \hat{\mathcal{S}}^z_{i+1} + \cos(2\theta)(\hat{\mathcal{S}}^x_i \hat{\mathcal{S}}^x_{i+1} + \hat{\mathcal{S}}^y_i \hat{\mathcal{S}}^y_{i+1})] + J \sin(2\theta) \sum_{i=1}^{N} (-1)^i (\hat{\mathcal{S}}^x_i \hat{\mathcal{S}}^y_{i+1} - \hat{\mathcal{S}}^y_i \hat{\mathcal{S}}^x_{i+1}) + g_\perp \mu_B B \sum_{i=1}^{N} \hat{\mathcal{S}}^x_i \Bigg\}. \tag{1}$$

The Dzyaloshinskii–Moriya interaction is eliminated by rotating the spins in the x–y plane by the angle θ [15]:

$$\begin{aligned} \hat{\mathcal{S}}^x_i &= \cos(\theta)\mathcal{S}^x_i + (-1)^i \sin(\theta)\mathcal{S}^y_i, \\ \hat{\mathcal{S}}^y_i &= -(-1)^i \sin(\theta)\mathcal{S}^x_i + \cos(\theta)\mathcal{S}^y_i, \\ \hat{\mathcal{S}}^z_i &= \mathcal{S}^z_i. \end{aligned} \tag{2}$$

Then the model is mapped onto [15]

$$\mathcal{H} = -J \sum_{i=1}^{N} \mathbf{S}_i \mathbf{S}_{i+1} - g_\perp \mu_B B^x \sum_{i=1}^{N} S^x_i - g_\perp \mu_B B^y_s \sum_{i=1}^{N} (-1)^i S^y_i, \tag{3}$$

where $B^x = B\cos(\theta)$, $B^y_s = B\sin(\theta)$ and B is the uniform external magnetic field perpendicular to the one-dimensional spin-chain. Eq. (3) describes the effective isotropic Heisenberg model with both the uniform field B^x and the transverse staggered field B^y_s. If the external magnetic field is applied along the spin-chain we replace $\theta = 0$ and $g_\perp = g_\parallel$ in Eq. (3).

The thermodynamical mean value of any quantity described by the self-adjoint operator $\mathcal{A}$ is given by

$$\langle \mathcal{A} \rangle = \frac{1}{\mathcal{Z}} \mathbf{Tr}\{\mathcal{A} e^{-\beta\mathcal{H}}\}, \quad \beta = \frac{1}{k_B T}, \tag{4}$$

where k_B – the Boltzmann constant and T – temperature in K. We may also calculate the thermodynamic properties from the derivatives of the free energy related to the partition function $\mathcal{Z}$. For the spin system described in (3) we can calculate the canonical partition function $\mathcal{Z}$ from the definition

$$\mathcal{Z} = \mathbf{Tr} e^{-\beta\mathcal{H}}. \tag{5}$$

The values of matrix elements of $e^{-\beta\mathcal{H}}$ cannot be calculated for large N because of non-commuting operators in (3). Thus, to eliminate this restriction, we look for systematic approximants to the partition function $\mathcal{Z}$.

We express Hamiltonian (3) as a sum of the spin-pair operators $\mathcal{H}_{i,i+1}$, where

$$\mathcal{H}_{i,i+1} = -J\mathbf{S}_i\mathbf{S}_{i+1} - \frac{1}{2} g_\perp \mu_B [B^x (S^x_i + S^x_{i+1}) + (-1)^i B^y_s (S^y_i - S^y_{i+1})]. \tag{6}$$

In the check-board decomposition (CBD) we divide the Hamiltonian (3) into two non-commuting parts [16]

$$\begin{aligned} \mathcal{H} &= \mathcal{H}^{\text{odd}} + \mathcal{H}^{\text{even}} \\ &= (\mathcal{H}_{1,2} + \cdots + \mathcal{H}_{N-1,N}) + (\mathcal{H}_{2,3} + \cdots + \mathcal{H}_{N,1}), \end{aligned} \tag{7}$$

each part defined by the commuting spin-pair operators $\mathcal{H}_{i,i+1}$. Then the series of the classical approximants of the quantum thermal values can be found, using the general Suzuki–Trotter formula [16]. The partition function is calculated from the expression

$$\mathcal{Z} = \lim_{m\to\infty} \mathcal{Z}_m = \lim_{m\to\infty} \mathbf{Tr} \left[\prod_{i=1}^{N/2} \mathcal{V}_{2i-1,2i} \prod_{i=1}^{N/2} \mathcal{V}_{2i,2i+1} \right]^m, \tag{8}$$

where $\mathcal{V}_{i,i+1} = e^{-\beta\mathcal{H}_{i,i+1}/m}$, $i = 1, 2, \ldots, N$ and m is a natural number (referred to as the Trotter number).

The approximant $\mathcal{Z}_m$ can be calculated numerically, without any restrictions on the value of N, by the quantum transfer-matrix (QTM) method. The computation of $\mathcal{Z}_m$ is possible for relatively small values of m, because of computer storage limitation, but the leading errors in taking a finite m approximant are of the order of $1/m^2$ and therefore, extrapolations to $m \to \infty$ can be performed.

For infinite chains (the macroscopic limit) it is better to reverse the transfer direction and to calculate the partition function from the largest eigenvalue of the transfer matrix. In order to reverse the transfer direction we must define a new local transfer matrix $\mathcal{L}_{r,r+1}$ whose elements depend on the local transfer matrix $\mathcal{V}_{i,i+1}$ elements:

$$\langle S^z_{r,i} S^z_{r+1,i} | \mathcal{L}_{r,r+1} | S^z_{r,i+1} S^z_{r+1,i+1} \rangle = \langle S^z_{r,i} S^z_{r,i+1} | \mathcal{V}_{i,i+1} | S^z_{r+1,i} S^z_{r+1,i+1} \rangle. \tag{9}$$

These operators act in a Hilbert space $\mathcal{H}^{2m}$ whose dimension is independent of N.

Now we define a unitary shift operator. In the case of the non-uniform spin chains we define also a unitary shift

operator $\mathscr{D}$, acting in the space $\mathscr{H}^{2m}$ which is a direct product of $2m$ single-spin spaces $\mathscr{H}^r$, similar to that for the uniform chain [16]

$$\mathscr{D} \equiv \sum_{S_1^z} \cdots \sum_{S_{2m}^z} |S_3^z \cdots S_{2m}^z S_1^z S_2^z\rangle\langle S_1^z S_2^z S_3^z \cdots S_{2m}^z|. \tag{10}$$

Using Eq. (10), we may express operators $\mathscr{L}_{r,r+1}$ in terms of the operators $\mathscr{L}_{1,2}$ and $\mathscr{L}_{2,3}$

$$\mathscr{L}_{2r-1,2r} = (\mathscr{D}^+)^{r-1}\mathscr{L}_{1,2}\mathscr{D}^{r-1},$$
$$\mathscr{L}_{2r,2r+1} = (\mathscr{D}^+)^{r-1}\mathscr{L}_{2,3}\mathscr{D}^{r-1}. \tag{11}$$

In this case the global transfer matrices can be expressed in terms of two operators $\mathscr{L}_{1,2}$ and $\mathscr{L}_{2,3}$:

$$\mathscr{W}_r = (\mathscr{L}_{r,r+1}\mathscr{D}^+)^m, \quad r = 1,2. \tag{12}$$

Finally, the mth classical approximant to the partition function can be written in the following form:

$$Z_m = Tr(\mathscr{W}_1\mathscr{W}_2)^{N/2}. \tag{13}$$

In the limit $N \to \infty$ the partition function $\mathscr{Z}$ is equal to the highest eigenvalue of the global transfer matrix $\mathscr{W} = \mathscr{W}_1\mathscr{W}_2$.

To calculate the partition function for finite chains we need to define the two vectors which act in the Hilbert space $\mathscr{H}^{2m}$ [16]:

$$|a\rangle = \sum_{\{S^z\}} \prod_{r=1}^{2m} \delta_{S_{2r-1}^z, S_{2r}^z} |S_1^z \cdots S_{2m}^z\rangle, \tag{14}$$

$$|b\rangle = \sum_{\{S^z\}} \prod_{r=1}^{2m} \delta_{S_{2r}^z, S_{2r+1}^z} |S_1^z \cdots S_{2m}^z\rangle. \tag{15}$$

Then the mth classical approximant to the partition function of Eq. (3) is of the form:

$$\mathscr{Z}_m = \langle b|(\mathscr{W}_1\mathscr{W}_2)^{(N-1)/2}|a\rangle \quad \text{for odd} \quad N, \tag{16}$$

$$\mathscr{Z}_m = \langle b|(\mathscr{W}_1\mathscr{W}_2)^{N/2-1}|a\rangle \quad \text{for even} \quad N. \tag{17}$$

The thermodynamic functions for all systems described by Hamiltonian (3) are related to the free energy which can be calculated from the formula $\mathscr{F} = -k_B T \ln \mathscr{Z}$. The specific heat is given as its second derivative with respect to temperature. Our approach is complementary with respect to the DMRG technique [15].

3. Simulation results and experimental data

The experiments were carried out on high-quality single crystals of the polydomain pure Yb_4As_3, prepared as described in Ref. [1] and diluted $(Yb_{1-x}Lu_x)_4As_3$ ($x = 0.01, 0.03$) samples. For the latter, the x values represent the nominal concentration. The comparison of $\chi(T)$ for the various doped samples with the respective $\chi(T)$ for undoped Yb_4As_3 in the temperature range between 10 and 40 K yields actual Lu concentrations which are very close (within 10%) to the nominal ones. For the specific heat measurements a microcalorimeter from Oxford Instruments was used.

In our simulations for pure Yb_4As_3 we adopt the literature parameters. The g-factors parallel and perpendicular to the spin chain of Yb_4As_3 were estimated as of about $g_{\|} = 2.9$ and $g_{\perp} = 1.3$ respectively, from the analysis of the scattering vector dependence of the inelastic response at zero field and the induced moment on the Yb^{3+} ions measured by polarised neutron diffraction under magnetic field [7]. An intrachain exchange coupling ($J/k_B = -26$ K) [4] was found from the uniform susceptibility measurements. The magnetization measurements led to the value $\tan(\theta) = 0.19$ [15] so that the uniform field is about five times stronger than the effective staggered field induced by the Dzyaloshinskii–Moriya interaction. Using this parameters we performed numerical simulations reported in [17]. In this paper we presented also numerical calculation results for $J/k_B = -30$ K.

The specific heat results for the $B = 0$ T and $B = 8$ T are shown in Fig. 1. The open symbols represent our experimental results for a polydomain sample in the absence magnetic field and with the magnetic field applied along the cubic $\langle 111\rangle$ direction [18]. The remaining symbols are numerical results. For the experimental data the phonon contribution $C_{ph} = 2.052 \times 10^{-3}\ T^3$ J/(K^4 mol) was subtracted [18]. The computer calculations were performed for a polydomain sample in which 25% of the domains were oriented with the spin chains parallel to the applied field B and about 75% of the domains were aligned so that the effective field component $B \cdot \sin(70°)$ was perpendicular to the spin chains.

Our theoretical data for $J/k_B = -26$ K (Fig. 1) systematically overestimate the experimental data [17] whereas these for $J/k_B = -30$ K are shifted in the proper direction. It shows a strong dependence of the results on this parameter. Apart from that, the discrepancy between the theoretical results and experimental data may be related to some

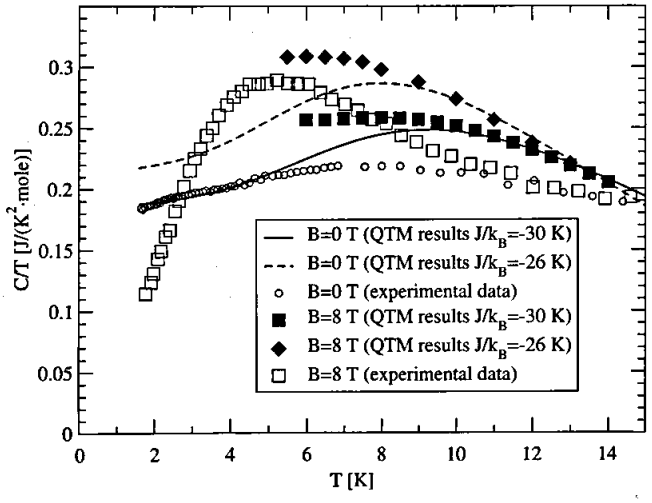

Fig. 1. Comparison of the measured specific heat after phonon subtraction and QTM calculation for Yb_4As_3. The lines and open circles represent zero-field specific heat and remaining symbols represent specific heat for finite magnetic fields $B = 8$ T.

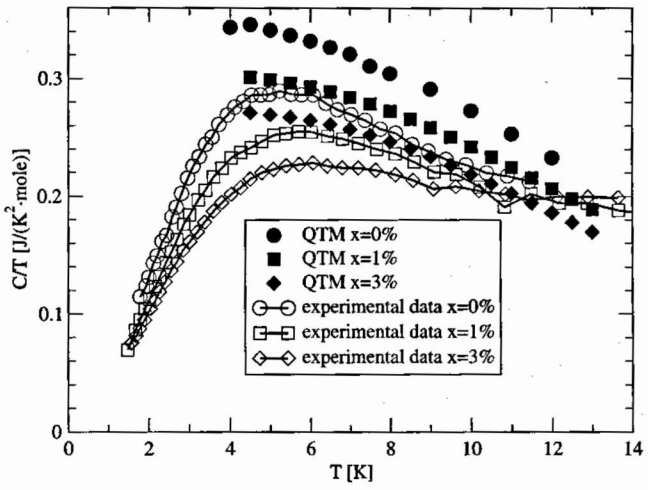

Fig. 2. Comparison of the QTM results (full symbols) and polydomain specific heat for Yb4As3 and $(Yb_{1-x}Lu_x)_4As_3$ (open symbols) under magnetic field $B = 12$ T.

uncertainty in the experimental subtraction of the lattice contribution.

Similar simulations ($J/k_B = -26$ K) were performed for diluted system and compared with specific heat experimental results for a polydomain sample $(Yb_{1-x}Lu_x)_4As_3$ ($x = 0.01$, 0.03) in the applied field $B = 12$ T. Assuming the uniform distribution of Lu–ions among the chains, each site in the Yb^{3+}-chain is randomly occupied by a magnetic ion with a probability $p = 1 - x$. The probability of one end having an empty neighbour is $(1 - p)$. The total probability that a fixed lattice site is the left end of an L-cluster is $p_L(1-p)^2$. The probability distribution of chains with L sites is $w_L = p^{L-1}(1-p)$. Then the specific heat per spin [19]:

$$C = \frac{n}{N}\sum_{L=1}^{\infty} w_L \cdot C_L, \tag{18}$$

where C_L denotes the specific heat of a finite chain with L sites, N is the number of all the spins in the system and n is the number of chains. We note that the specific heat per a molecule of $(Yb_{1-x}Lu_x)_4As_3$ is given as $(1-x)\cdot C$ and finally we have

$$C = x^2 \cdot \sum_{L=1}^{\infty}(1-x)^L \cdot C_L. \tag{19}$$

In Fig. 2 we compare specific heat experimental results for a polydomain diluted and pure sample in the applied field $B = 12$ T and numerical data for the finite chain assuming $J/k_B = -26$ K. Our theoretical specific-heat data systematically overestimate the experimental results but reveal qualitative agreement with experiment. The same behaviour was observed previously for the pure system (Fig. 2 in [17]).

4. Conclusions

We have presented experimental data of zero-field and field-dependent specific heat mesurements for pure and diluted polydomain Yb_4As_3 sample. We have worked out the QTM approach to compare numerical results with experimental data. The QTM calculations for pure Yb_4As_3 have been performed for the Heisenberg model with the Dzyaloshinskii–Moriya interaction, using two different exchange integrals $J/k_B = -26$ K and $J/k_B = -30$ K. For the diluted $(Yb_{1-x}Lu_x)_4As_3$ ($x = 0.01$, 0.03) systems, for the first time, we have considered the random impurity distribution, revealing the qualitative agreement with experiment. In order to obtain better agreement between the model calculations and experimental data for both pure and diluted system, probably the estimates of exchange coupling and phonon contribution should be reconsidered. However it seams impossible to achieve due to discrepancies in the existing low-temperature specific heat data [2,5,18] for the pure compound.

Acknowledgements

We thank Mr. Kamil Rachwał for some technical help. This work was supported by the Polish Ministry of Science and Education Grant 4 T11F 014 24 and the UE NoE project NMP3-CT-2005-515767. Computations were partially performed on PCSN supercomputing platforms.

References

[1] A. Ochiai, T. Suzuki, T. Kasuya, J. Phys. Soc. Jpn. 59 (1990) 4129.
[2] M. Köppen, M. Lang, R. Helfrich, F. Steglich, P. Thalmeier, B. Schmidt, B. Wand, D. Pankert, H. Benner, H. Aoki, A. Ochiai, Phys. Rev. Lett. 82 (1999) 4548.
[3] V.N. Antonov, A.N. Yaresko, A.Ya. Perlov, P. Thalmeier, P. Fulde, P.M. Openeer, H. Eschrig, Phys. Rev. B 58 (1998) 9752.
[4] M. Kohgi, K. Iwasa, J.-M. Mignot, A. Ochiai, T. Suzuki, Phys. Rev. B 56 (1997) R11388.
[5] B. Schmidt, H. Aoki, T. Cichorek, J. Custers, P. Gegenwart, M. Kohgi, M. Lang, C. Langhammer, A. Ochiai, S. Paschen, F. Steglich, T. Suzuki, P. Thalmeier, B. Wand, A. Yaresko, Physica B 300 (2001) 121.
[6] P. Fulde, B. Schmidt, P. Thalmeier, Europhys. Lett. 31 (1995) 323.
[7] M. Kohgi, K. Iwasa, J.-M. Mignot, B. Fak, P. Gegenwart, M. Lang, A. Ochiai, H. Aoki, T. Suzuki, Phys. Rev. Lett. 86 (2001) 2439.
[8] M. Oshikawa, I. Affleck, Phys. Rev. Lett. 79 (1997) 2883.
[9] D.C. Dender, P.R. Hammar, Daniel H. Reich, C. Broholm, G. Aeppli, Phys. Rev. Lett. 79 (1997) 1750.
[10] R. Feyerherm, S. Abens, D. Günther, T. Ishida, M. Meißner, M. Meschke, T. Nogami, J. Phys.: Condens. Matter. 12 (2000) 8495.
[11] M. Oshikawa, I. Affleck, Phys. Rev. Lett. 82 (1999) 5136.
[12] S. Bertaina, V.A. Pashchenko, A. Stepanov, T. Masuda, K. Uchinokura, Phys. Rev. Lett. 92 (2004) 057203.
[13] M. Oshikawa, K. Ueda, H. Aoki, A. Ochiai, M. Kohgi, J. Phys. Soc. Jpn. 68 (1999) 3181.
[14] H. Shiba, K. Ueda, O. Sakai, J. Phys. Soc. Jpn. 69 (2000) 1493.
[15] N. Shibata, K. Ueda, J. Phys. Soc. Jpn. 70 (2001) 3690.
[16] T. Delica, H. Leschke, Physica A176 (1990) 736.
[17] G. Kamieniarz, R. Matysiak, P. Gegenwart, H. Aoki, A. Ochiai, J. Magn. Magn. Mater. 290–291 (2005) 353.
[18] P. Gegenwart, H. Aoki, T. Cichorek, J. Custers, N. Harrison, M. Jaime, M. Lang, A. Ochiai, F. Steglich, Physica B 312–313 (2002) 315.
[19] H. Asakawa, M. Matsuda, K. Minami, H. Yamazaki, K. Katsumata. Phys. Rev. B 57 (1998) 8285.